

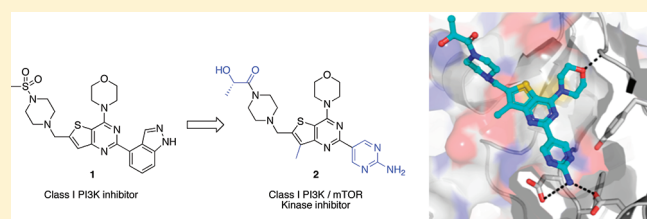
Discovery of a Potent, Selective, and Orally Available Class I Phosphatidylinositol 3-Kinase (PI3K)/Mammalian Target of Rapamycin (mTOR) Kinase Inhibitor (GDC-0980) for the Treatment of Cancer

Daniel P. Sutherland,^{*,†} Linda Bao,[†] Megan Berry,[†] Georgette Castanedo,[†] Irina Chuckowree,[‡] Jenna Dotson,[†] Adrian Folks,[‡] Lori Friedman,[†] Richard Goldsmith,[†] Janet Gunzner,[†] Timothy Heffron,[†] John Lesnick,[†] Cristina Lewis,[†] Simon Mathieu,[†] Jeremy Murray,[†] Jim Nonomiya,[†] Jodie Pang,[†] Niel Pegg,[‡] Wei Wei Prior,[†] Lionel Rouge,[†] Laurent Salphati,[†] Deepak Sampath,[†] Qingping Tian,[†] Vickie Tsui,[†] Nan Chi Wan,[‡] Shumei Wang,[†] BinQing Wei,[†] Christian Wiesmann,[†] Ping Wu,[†] Bing-Yan Zhu,[†] and Alan Olivero[†]

[†]Genentech, Inc., 1 DNA Way, South San Francisco, California 94080, United States

[‡]Piramed Pharma, 957 Buckingham Avenue, Slough, Berks SL1 4NL, United Kingdom

ABSTRACT: The discovery of **2** (GDC-0980), a class I PI3K and mTOR kinase inhibitor for oncology indications, is described. mTOR inhibition was added to the class I PI3K inhibitor **1** (GDC-0941) scaffold primarily through the substitution of the indazole in **1** for a 2-aminopyrimidine. This substitution also increased the microsomal stability and the free fraction of compounds as evidenced through a pairwise comparison of molecules that were otherwise identical. Highlighted in detail are analogues of an advanced compound **4** that were designed to improve solubility, resulting in **2**. This compound, is potent across PI3K class I isoforms with IC₅₀s of 5, 27, 7, and 14 nM for PI3K α , β , δ , and γ , respectively, inhibits mTOR with a K_i of 17 nM yet is highly selective versus a large panel of kinases including others in the PIKK family. On the basis of the cell potency, low clearance in mouse, and high free fraction, **2** demonstrated significant efficacy in mouse xenografts when dosed as low as 1 mg/kg orally and is currently in phase I clinical trials for cancer.



INTRODUCTION

Both PI3K and mTOR have been identified as promising kinase targets for the treatment of cancer. These enzymes participate in related, but not redundant, signaling networks to transmit cellular growth and survival signals, which are hallmarks of tumor growth.^{1–5} An interest in targeting two important points along this critical signaling pathway, along with the fact that PI3Ks and mTOR have a high degree of active site similarity, has spurred the development of PI3K/mTOR inhibitors for oncology indications.^{6–8}

PI3K α , a member of the class I PI3Ks (α , β , δ , γ), has been linked to cancer through the identification of activating mutations in the kinase domain,^{9–12} loss of function mutations in the PI3K negative regulator PTEN,^{13,14} through its key role in transmitting signals to or from known oncogenes (such as EGFR, HER2, RAS, and AKT)^{1,2} and as a recognized mechanism for resistance to known therapies.¹⁵ Functionally, this lipid kinase is responsible for the phosphorylation of phosphatidylinositol (4,5) bis-phosphate to phosphatidylinositol (3,4,5) tris-phosphate, which then recruits additional kinases to the membrane, activating the oncogene AKT. AKT, in turn is then responsible for a broad number of downstream signaling events that includes mTOR activation. Several class I PI3K inhibitors, including **1**

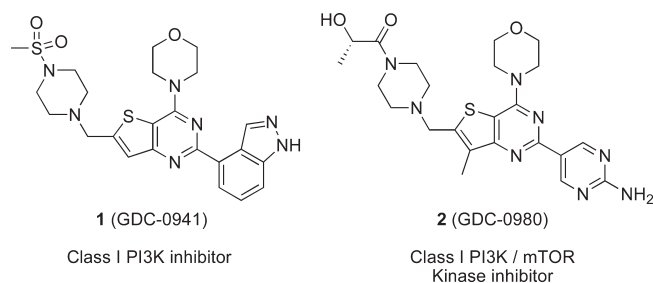


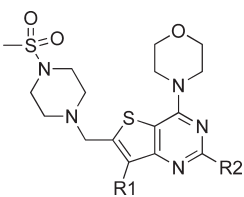
Figure 1. Structures of morpholino thienopyrimidine inhibitors of class I PI3Ks, **1**, and class I PI3Ks and mTOR Kinase, **2**.

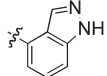
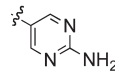
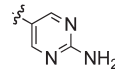
(GDC-0941, Figure 1),^{16,17} have entered clinical trials. Additionally, isoform selective compounds have also entered clinical development for various oncology indications.¹⁸

The kinase mTOR, a member of the PIKK (phosphatidylinositol like kinase) family, is activated downstream of AKT and leads to increased protein synthesis and growth.⁵ Rapamycin analogues such as temsirolimus, which inhibits mTOR when complexed in

Received: July 13, 2011

Published: October 07, 2011

Table 1. Relevant Potency and PK Data for Previously Described Molecules 1, 3, and 4^a


Comp	R1	R2	IC ₅₀ or K _{i app} * (nM)				thermodynamic solubility			
			p110α	mTOR*	PC3 cell	MCF7 -neo/HER2 cell	rat Cl _p (ml/min/kg)	dog Cl _p (ml/min/kg)	PPB human	pH6.5 (μg/mL)
1	H		3	580	280	290	60	12	93%	16
3	H		2	29	310	130	24	22	51%	24
4	CH ₃		4	21	220	143	13	5	77%	9

^a Male Sprague–Dawley rats and male beagle dogs were dosed intravenously at 1 mg/kg for rat and dog (1 rat, dimesylate salt in 5% DMSO, 5% cremaphore (5 mg/kg); dog, dimesylate salt in 30% SBE-β-CD. 3 rat, TFA salt in 5% DMSO, 5% cremaphore; dog, HCl salt in 20% HP-β-CD. 4 rat, TFA salt in 5% DMSO, 5% cremaphore; dog, HCl salt in 10% HP-β-CD). *K_{i app} is reported for mTOR, all others are IC₅₀s.^{16,31,32}

part to rictor (mTORC1 complex), have been approved for the treatment of advanced renal cell carcinoma and mantle cell lymphoma, validating this target in humans.¹⁹ One potential limitation of exclusive mTORC1 inhibition by rapamycin analogues are that mTOR kinase also participates in the mTORC2 protein complex that can activate the oncogene AKT, through phosphorylation of AKT Ser473, and promote cell survival through other signaling mechanisms.²⁰ Experimentally, it has been shown that inhibition of mTORC1 by rapamycin analogues fails to repress a negative feedback loop that results in the phosphorylation and activation of AKT.^{21–24} To avoid this undesired feedback mechanism and potential to reactivate the pathway and cause resistance, ATP competitive mTOR kinase inhibitors that can inhibit both mTORC1 and mTORC2 have been pursued as alternatives to the rapamycin analogues.²⁵

Given the quantity of evidence implicating both PI3K and mTOR in cancer, we and others have developed compounds that inhibit both kinases. Several of these inhibitors have begun early clinical development.^{26–29} The discovery of 2 (GDC-0980), also in the clinic, is described herein. By inhibiting two nodes in this critical pathway, this compound may provide a therapeutic advantage relative to inhibitors that target PI3K or mTOR alone.

RESULTS AND DISCUSSION

The class I PI3K inhibitor 1 served as a useful template to explore the potential addition of mTOR potency, as this compound possessed good potency, was selective against a large panel of kinases, and was efficacious in mice xenograft studies when dosed orally.¹⁶ At the outset of our work, it was known that the tool compound PI-103, also possessing a morpholino pyrimidine core, did inhibit mTOR and PI3Ks, and it was conceivable that mTOR potency could be acquired through modification of 1.³⁰ Secondary to this effort, we aimed to improve clearance of

the scaffold while also maintaining or improving potency and solubility.

Recent communications from our lab have described the discovery of the 2-aminopyrimidyl-thienopyrimidine 3 and the 7-methyl analogue 4 (Table 1).^{31–33} These compounds are potent inhibitors of mTOR and the class I PI3Ks and confirm the potential to inhibit both kinases in this structural class. In addition to biochemical assays, these compounds are also potent in cell-based proliferation assays where human tumor cell growth is driven by loss of the negative regulator PTEN (PC3 line) or activating mutations in PI3Kα (MCF7-neo/HER2 line). Proliferation IC₅₀s correlated well with cellular pAKT IC₅₀s measured in PC3 cells, a downstream readout of pathway inhibition (correlation coefficients of 0.78 and 0.74 for the PC3 and MCF7-neo/HER2 lines, respectively, when looking across >200 compounds from multiple scaffolds). The replacement of the indazole with a 2-aminopyrimidine, found in 1 and 3, respectively, was a key factor in increasing potency for mTOR by 10-fold on average across a number of diverse morpholino thienopyrimidines. When this change was applied to the lead compound 1 to generate 3, the result was a 20-fold improvement in mTOR inhibition. Proliferation IC₅₀s for potent PI3Kα inhibitors were not dramatically affected by additional mTOR inhibition in these two specific cell lines. This observation was not surprising in that these two lines used in the discovery phase of the program depended exclusively on PI3Kα activity for growth.

In addition to the increased mTOR inhibition brought about through the aminopyrimidine substitution, the cLogP of the scaffold was lowered by 1.9 units via this change and consequently increased the free fraction and the in vitro stability of the molecules across species (measured logDs for 1 and 3 were 2.4 and 1.3, respectively). To systematically observe these effects, we examined matched pairs of compounds where the core and pendant R groups are held constant and the data is compared

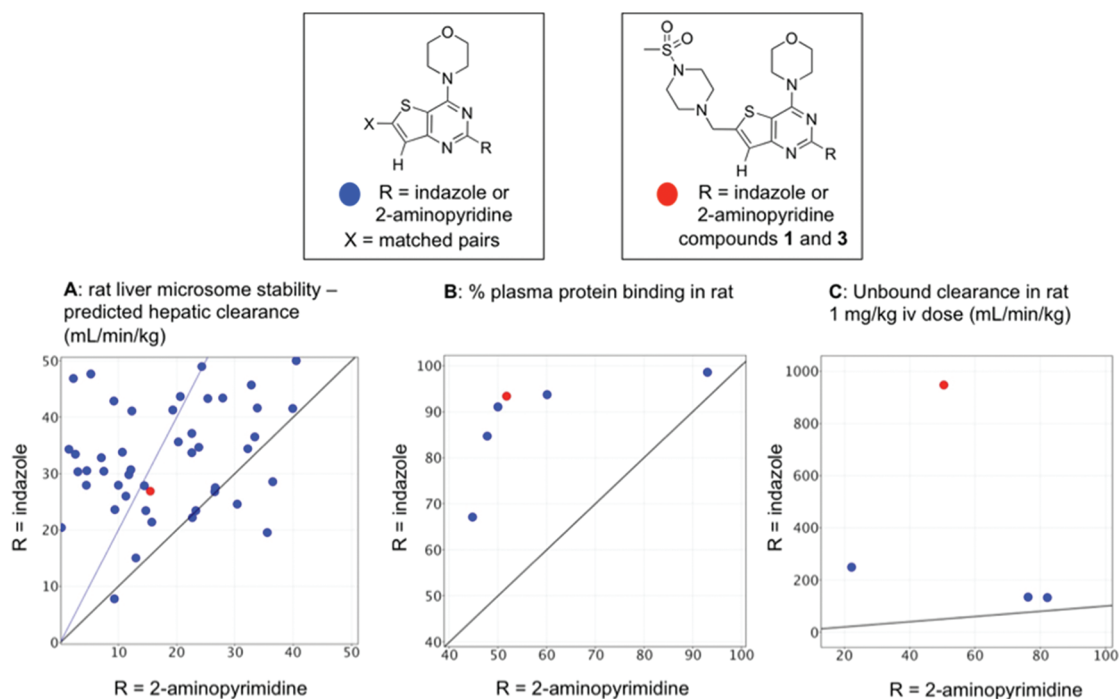
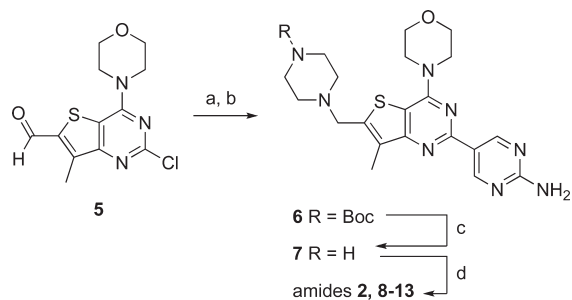


Figure 2. Comparisons of rat liver microsome stability, plasma protein binding, and unbound clearance in rat for matched pairs of compounds having either an indazole or a 2-aminopyrimidine. Points on each graph represents two compounds where R = indazole (data on the y axis) or R = 2-aminopyrimidine (x axis). Blue points have undisclosed X groups, and the red point indicates the data for compounds **1** and **3** specifically. The black lines represent the line of unity, and the blue line in (A) represents a 2-fold change from the line of unity. Hepatic clearance in (A) was predicted from liver microsome incubations using the “in vitro $t_{1/2}$ method”.³⁵

Scheme 1. Synthesis of Compounds Found in Table 2^a

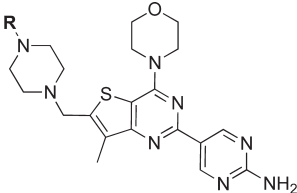


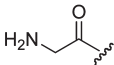
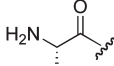
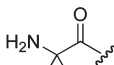
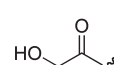
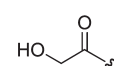
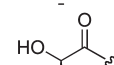
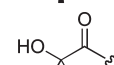
^a Reagents and conditions: (a) Boc-piperazine, 1,2-DCE, $\text{HC}(\text{OCH}_3)_3$, $\text{Na}(\text{OAc})_3\text{BH}$, 96%; (b) 2-aminopyrimidine-5-boronic acid pinacol ester, $\text{Pd}(\text{PPh}_3)_2\text{Cl}_2$, 1 M Na_2CO_3 , CH_3CN , microwave, 140 °C, 15 min, 82%; (c) 4N HCl in dioxane, DCM, 25 °C, 3 h, 100%; (d) RCOOH , DIPEA, HATU, DMF, 25 °C, 30 min, 42–56%.

exclusively between the indazole and the aminopyrimidine (Figure 2A–C). Figure 2A shows that when 46 indazole/pyrimidine matched pairs are compared, 21 of the pyrimidines were >2 fold more stable than the corresponding indazole-containing analogue in rat liver microsomes. The remaining 30 compounds are within an accepted 2-fold margin of error for this assay. Additionally, for the comparisons that can be made, the PPB in rat is also lowered significantly for all compounds (Figure 2B). These findings were not restricted to rat and could be seen across species, including human (data not shown). The increased microsomal stability correlated well with in vivo data and contributed to equivalent or significantly lower unbound clearances for all molecules tested in rat (Figure 2C).

Where **3** displayed good clearance in rats, methyl substitution of the core found in **4** was required to give low clearances in dogs as well. While this change improved dog clearances, compounds such as **4** suffered from relatively low solubility and was considered to increase the compounds potential risk of solubility limited exposure and PK variability in humans. Thus, the focus of further work was to determine whether analogues could be generated with better solubility while maintaining the biological and pharmacokinetic properties of **4**. With this goal in mind, we considered solubility improvements to be best accessed through modification of the solvent exposed sulfonamide found on the piperazine ring. This was thought to be possible due to the added potency afforded by the 2-aminopyrimidine that allowed greater flexibility in the SAR surrounding the solvent exposed region of the core.³¹

Chemistry. Piperazine amides **2** and **8–13** (Scheme 1 and Table 2) were pursued to maintain the neutral charge of the distal nitrogen of the piperazine ring to provide a balance of polarity without added molecular weight and to utilize readily available amino acid starting materials. We explored both amino and hydroxy acids to improve solubility and with and without substitution at the α carbon to modulate metabolic stabilities. Synthetically, the amides were installed in the last step due to instability of this group to the high temperature Suzuki reaction used to install the aminopyrimidine. Unsubstituted piperazine **7** was generated from the previously described aldehyde **5** after reductive amination with Boc-piperazine, Suzuki coupling with 2-aminopyrimidine-4-boronic acid, and Boc deprotection of **6**. The final products were made with Boc protected amino acids which were deprotected following coupling or with the unprotected hydroxy acids to give **2** and **8–13**.

Table 2. Biochemical and Cell-Based Potency, Predicted and in Vivo Hepatic Clearances, and Thermodynamic Solubility for Compounds 2 and 8–13^a


Compound	R	IC ₅₀ or K _{i app} * (nM)					Clearance (ml/min/kg)			thermodynamic solubility	
		p110α	mTOR*	p110β/δ/γ	PC3	MCF7	human pred. Cl _h	rat pred. Cl _h	Rat Cl _p	F%	pH 6.5 (mg/mL)
8		0.7	12	11/4.3/17	228	518	10.8	16.1	140	0	0.69
9		2.1	6.3	29/2.4/37	556	472	7.1	6.7	-	-	-
10		1.0	14	44/1.5/20	367	289	8.6	19.2	84	6	1.0
11		2.8*	-	19/5.6/10	457	288	4.1	3.6	-	-	-
2		4.8	17	27/6.7/14	307	255	3.1	4.4	15	100	0.084
12		8.7	-	145/11/33	295	356	6.5	11	17	77	-
13		1.7	14	45/5.0/25	116	161	7.2	13.7	24	71	0.6

^a Male Sprague–Dawley rats were dosed with TFA salts of each compound intravenously at 1 mg/kg as a solution in 5% DMSO/5% cremophor and dosed orally in 80% PEG400 (or 0.5% methylcellulose)/0.2% Tween-80 for compound 2). *K_{i app} is reported for mTOR and PI3Kα for compound 11, all others are IC₅₀s. Hepatic clearance was predicted from liver microsome incubations using the “in vitro t_{1/2} method”.³⁵

A subset of structurally related analogues are shown in Table 2. The amine-based glycine, alanine, and dimethyl glycine derivatives of 4 all had respectable potencies in biochemical and cell-based assays along with the desired significant improvements in thermodynamic solubility at pH 6.5. However, in vivo clearance for the two analogues tested, 8 and 10, were at or above liver blood flow³⁴ and the compounds had little or no oral bioavailability. The alcohol-based analogues had much better PK properties as exemplified by 2, 12, and 13, which had increased solubility, low to moderate clearance, and good oral bioavailability. Compound 11 was not advanced further as the cellular potency in the PC3 line was above 400 nM. Lactic amide 12 had biochemical potencies and human microsomal stabilities that were less preferred relative to its enantiomer 2, even though rodent PK and cellular potencies were roughly similar. Lactic amide 2 was chosen for further study primarily due to its low predicted clearance in human as measured in vitro with human liver microsomes, its low in vivo clearance in rat, and maximized oral bioavailability relative to tertiary alcohol 13. In addition to measuring cellular proliferation in the PC3 line, direct inhibition of PI3K could be monitored in these same cells by monitoring

the phosphorylation of Ser473 on AKT. In this assay, 2 had an IC₅₀ of 36 nM. Additionally, to confirm the binding mode of 2, we obtained a cocrystal structure of this compound bound to PI3Kγ (Figure 3). The structure bound in accordance with a similar previously disclosed amino-pyridine.³¹

Kinase Selectivity. Previous PI3K inhibitors from this and other chemical classes have maintained a high degree of selectivity over off-target kinases even while maintaining dual inhibition for mTOR and the PI3K isoforms. To confirm this, 2 was submitted for screening in a panel of kinases provided by Invitrogen's SelectScreen service. Of the 240 total kinases in the SelectScreen panel, only 5 kinases other than the PI3K isoforms and mTOR consistently displayed greater than 60% inhibition when treated with 1 μM of 2: Fgr, Mlk1, PAK4, Syk, and Yes1. Measurement of IC₅₀s for the most potently inhibited kinases in the panel revealed significantly weaker values for the off-target kinases compared to PI3K/mTOR; IC₅₀s for Fgr, Mlk1, and Syk were 697, 232, and 134 nM, respectively. Compound 2 was also remarkably selective for several other members of the closely related PIKK family kinases: C2alpha IC₅₀ = 1300 nM; C2beta IC₅₀ = 794 nM; VPS34 IC₅₀ = 2000 nM;

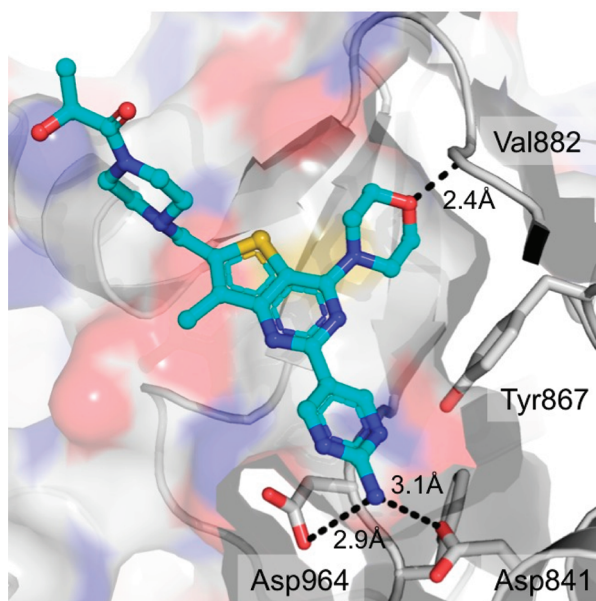


Figure 3. Crystal structure (2.8 Å) of **2** bound to PI3K γ . The backbone atoms of PI3K γ are shown in a cartoon representation with carbon atoms colored gray, **2** is shown in ball and stick representation with carbon atoms colored cyan. Critical contacts include the morpholine oxygen with the hinge residue Val882 and key contacts from the aminopyrimidine NH₂ to the carbonyl oxygens of Asp841 and Asp964. Crystals were grown at 18 °C from 20% PEG 3350, 0.2 M NH₄SO₄ by hanging drop vapor diffusion.¹⁶

PI4K α >10 μ M; PI4K β >10 μ M; DNA-PK K_{iapp} = 623 nM, respectively. Thus, the biochemical data illustrate that **2** had the desired selectivity profile, with potent inhibition of all class I PI3K isoforms and mTOR and selectivity over the other profiled PIKK family enzymes and a large, diverse panel of kinases.

Pharmacokinetics. On the basis of this promising profile, **2** was further characterized through PK studies conducted in several preclinical species. PK parameters obtained in mice after intravenous administration at 1 mg/kg and when dosed orally at 5 and 50 mg/kg are highlighted in Table 3 and are relevant to xenograft studies discussed herein. Clearance and PPB were low, and **2** showed dose-proportional exposure from 5 mg/kg dosed in PEG to 50 mg/kg dosed in suspension in MCT, a finding attributed partially to the compound's good solubility. PK parameters for **2** were also favorable in the other species tested, including dog (data not shown, manuscript in preparation). Plasma protein binding was similar across species.

In Vivo Efficacy. We evaluated the efficacy of compound **2** in vivo using xenografts derived from the same two tumor cell lines that were used to screen for cellular potency: PC-3 and MCF-7 neo/HER2 (Figure 4). The compound was dosed orally as a crystalline suspension in 0.5% methylcellulose/0.2% Tween-80 (MCT) once a day for either 14 or 22 days, and the tumor volume was measured relative to control animals treated with MCT vehicle only. In both PC-3 and MCF-7 neo/HER2 xenograft models, treatment with 1 mg/kg of compound **2** resulted in statistically significant antitumor activity, characterized as tumor growth delay [$p < .001$ vs vehicle treated group based on Dunnett's t test on day 14 (for PC3) and day 22 (for MCF-7 neo/HER2)]. At the maximum tolerated dose of 7.5 mg/kg, compound **2**, tumor stasis or regressions were observed in the PC-3 and MCF-7 neo/HER2 xenograft models, respectively [$p < .0001$ vs

Table 3. Pharmacokinetic and Plasma Protein Binding Data for Compound **2** in Mouse^a

predicted Cl _h (mL/min/kg)	IV (1 mg/kg)		PO				
	Cl _p (mL/min/kg)	V _{ss} (L/kg)	dose (mg/kg)	C _{max} (μ M)	AUC (μ M·h)	F %	PPB %
33	9.2	1.7	5	2.0	10	56	71
			50	24	121	66	

^a Female nu/nu mice were dosed with the HCl salt, either intravenously as a solution in 5% DMSO/5% cremophor, orally at 5 mg/kg in 80% PEG400, and orally at 50 mg/kg as a crystalline suspension in 0.5% methylcellulose/0.2% Tween-80. Hepatic clearance was predicted from mouse liver microsome incubations using the "in vitro $t_{1/2}$ method".³⁵

vehicle treated group based on Dunnett's t test on day 14 (for PC3) and day 22 (for MCF-7 neo/HER2)]. The significant antitumor activity of compound **2** at low doses is likely due to high cellular potency, low plasma clearance, and relatively high free fraction of the drug in vivo.

CONCLUSION

A potent and selective inhibitor of class I PI3 kinases and mTOR kinase was developed using lead compound **1** as a structural template. The replacement of an indazole with a 2-aminopyrimidine was responsible for increased potency for mTOR, lower PPB, and improved predicted and measured total and unbound clearances in rats and mice. A methyl group was added to the thienopyrimidine core to lower the in vivo clearances in rats and dogs further. Finally, a lactic amide was used to replace a sulfonamide in order to increase the thermodynamic solubility at a neutral pH, resulting in the discovery of **2**. On the basis of the potency for PI3K and mTOR, selectivity against other kinases, pharmacokinetics, solubility, and efficacy in PI3K driven animal models of cancer, this compound was advanced into development where it is currently in phase I clinical trials.

EXPERIMENTAL SECTION

Chemistry. All solvents and reagents were used as obtained. ¹H NMR spectra were recorded with a Bruker Avance DPX400 spectrometer or a Varian Inova 400 NMR spectrometer and referenced to tetramethyl silane. Chemical shifts are expressed as δ units using tetramethylsilane as the external standard (in NMR description, s, singlet; d, doublet; t, triplet; q, quartet; m, multiplet; and br, broad peak). Mass spectra were measured with a Finnigan SSQ710C spectrometer using an ESI source coupled to a Waters 600MS HPLC system operating in reverse mode with an X-bridge Phenyl column of dimensions 150 mm by 4.6 mm, with 5 μ m sized particles. All compounds were purified to $\geq 95\%$ purity using reversed phase HPLC.

2-Chloro-7-methyl-4-morpholinothieno[3,2-d]pyrimidine-6-carbaldehyde (5). To 4-(2-Chloro-7-methylthieno[3,2-d]pyrimidin-4-yl)morpholine (3.18 g, 11.8 mmol) in THF (65 mL) at -78 °C

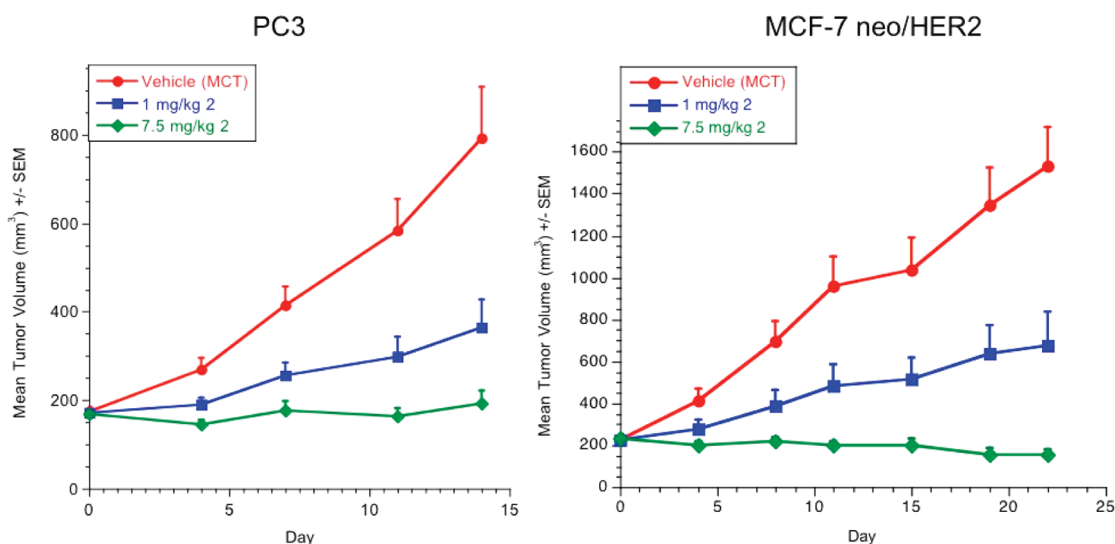


Figure 4. In vivo efficacy for **2** in PC3 and MCF-7 neo/HER2 xenograft tumor models when dosed orally at 1 and 7.5 mg/kg on a once daily schedule.

was added a 2.5 M solution of *n*-butyllithium in hexane (10.3 mL). The resulting solution was warmed to -40°C and stirred 2 h. DMF (4.2 mL, 54.2 mmol) was added, and the reaction mixture stirred 2 h at -40°C . The reaction was quenched by pouring slowly onto 0.25 M HCl with ice. After 1 h, the solid was filtered and lyophilized to yield 3.44 g of (**5**). ^1H NMR (400 MHz, CDCl_3) δ 10.32 (s, 1H), 4.02 (m, 4H), 3.79 (m, 4H), 2.68 (s, 3H). MS: (ESI+) 298.1.

tert-Butyl 4-((2-chloro-7-methyl-4-morpholinothieno[3,2-*d*]pyrimidin-6-yl)methyl)piperazine-1-carboxylate. 2-Chloro-7-methyl-4-morpholinothieno[3,2-*d*]pyrimidine-6-carbaldehyde (0.58 g) and *tert*-butyl piperazine-1-carboxylate (0.52 g) were dissolved in 1,2-dichloroethane (10 mL). Acetic acid (1.22 mL) was added and the reaction stirred 15 min before the addition of sodium triacetoxyborohydride (0.55 g). The resulting solution was stirred 24 h at room temperature. The reaction mixture was quenched with saturated aqueous NaHCO_3 , extracted with CH_2Cl_2 , dried over Na_2SO_4 , filtered, and concentrated in vacuo. The crude material was purified by flash chromatography (EtOAc/hexanes) to provide 880 mg of *tert*-butyl 4-((2-chloro-7-methyl-4-morpholinothieno[3,2-*d*]pyrimidin-6-yl)methyl)piperazine-1-carboxylate. ^1H NMR (400 MHz, DMSO) δ 3.88 (m, 4H), 3.82 (s, 2H), 3.74 (m, 4H), 3.34 (m, 4H), 2.43 (m, 4H), 2.23 (s, 3H), 1.39 (s, 9H). MS: (ESI+) 468.3.

tert-Butyl 4-((2-(2-Aminopyrimidin-5-yl)-7-methyl-4-morpholinothieno[3,2-*d*]pyrimidin-6-yl)methyl)piperazine-1-carboxylate (6**).** *tert*-Butyl 4-((2-chloro-7-methyl-4-morpholinothieno[3,2-*d*]pyrimidin-6-yl)methyl)piperazine-1-carboxylate (2.74 g, 5.8 mmol) was combined with bis(triphenylphosphine)palladium(II) chloride (0.21 g) and 2-aminopyrimidine-5-boronic acid pinacol ester (1.68 g) in 12 mL of acetonitrile and 12 mL of 1 M sodium carbonate in water. The reaction mixture was heated in a 50 mL microwave vessel and microwaved at 300 W to 140°C for 12 min. After cooling to room temperature, the resultant gray solid was washed with water and acetonitrile before solubilizing in a mixture of DMF, methanol, and DCM and stirred with charcoal overnight prior to filtering. This filtrate was treated with florisil for 2 h, filtered, and evaporated to give **6** as an off-white solid (2.52 g). ^1H NMR (400 MHz, DMSO) δ 9.15 (s, 2H), 7.06 (s, 2H), 3.97–3.91 (m, 4H), 3.83 (s, 2H), 3.80–3.74 (m, 4H), 3.34 (brs, 4H), 2.48–2.41 (m, 4H), 2.35 (s, 3H), 1.40 (s, 9H). MS: (ESI+) 527.2.

(7-Methyl-4-morpholino-6-(piperazin-1-ylmethyl)thieno[3,2-*d*]pyrimidin-2-yl)pyrimidin-2-amine (7**).** *tert*-Butyl 4-((2-(2-aminopyrimidin-5-yl)-7-methyl-4-morpholinothieno[3,2-*d*]pyrimidin-6-yl)methyl)piperazine-1-carboxylate (**6**) (9.0 g) was dissolved in 43 mL

of 4 M HCl in 1,4-dioxane and stirred for 3 h. The solution was evaporated and dried overnight under vacuum to afford **7** in 100% yield. NMR (400 MHz, DMSO) δ 9.15 (s, 2H), 7.06 (s, 2H), 4.05–3.86 (m, 4H), 3.85–3.69 (m, 6H), 2.70 (brs, 4H), 2.42 (brs, 4H), 2.34 (s, 3H). MS: (ESI+) 427.2.

2-Amino-1-(4-((2-(2-aminopyrimidin-5-yl)-7-methyl-4-morpholinothieno[3,2-*d*]pyrimidin-6-yl)methyl)piperazin-1-yl)ethanone (8**).** *N,N*-Diisopropylethylamine (150 μL , 0.87 mmol) was added to a solution of 5-(7-methyl-4-morpholino-6-(piperazin-1-ylmethyl)thieno[3,2-*d*]pyrimidin-2-yl)pyrimidin-2-amine **7** (74 mg, 0.17 mmol) in DMF (1 mL). HATU (97 mg, 0.26 mmol) and Boc-glycine (60 mg, 0.3 mmol) was added to the reaction mixture, which was stirred for 30 min at room temperature. The reaction mixture was diluted with ethyl acetate (10 mL) and extracted with a saturated sodium bicarbonate solution (10 mL). The organic layer was dried with magnesium sulfate, filtered, and then concentrated to afford the penultimate product. This intermediate was then subjected to a Boc-deprotection with TFA before final reverse-phase HPLC purification to give 75.3 mg (56%) of **8** ($2\times$ TFA salt) as a white solid. ^1H NMR (400 MHz, DMSO) δ 9.18 (s, 2H), 8.03 t, $J = 5.2$ Hz, 3H), 7.15 (brs, 2H), 4.00–3.94 (m, 4H), 3.89 (q, $J = 5.2$ Hz, $J = 10.8$ Hz, 2H), 3.82–3.76 (m, 4H), 3.51 (br m, 4H), 2.89 (br m, 4H), 2.42 (s, 3H). MS: (ESI+) 484.1.

(S)-2-Amino-1-(4-((2-(2-aminopyrimidin-5-yl)-7-methyl-4-morpholinothieno[3,2-*d*]pyrimidin-6-yl)methyl)piperazin-1-yl)propan-1-one (9**).** Compound **9** was prepared from intermediate **7** and Boc-L-alanine by the procedure for compound **8** in 42% yield. ^1H NMR (400 MHz, DMSO) δ 9.18 (s, 2H), 8.09 (d, $J = 3.8$ Hz, 3H), 7.10 (br s, 2H), 4.43–4.32 (m, 1H), 4.25 (br s, 2H), 4.01–3.93 (m, 4H), 3.83–3.75 (m, 5H), 3.62 (br m, 4H), 2.89 (br m, 4H), 2.42 (s, 3H), 1.31 (d, $J = 6.8$ Hz, 3H). MS: (ESI+) 498.1.

2-Amino-1-(4-((2-(2-aminopyrimidin-5-yl)-7-methyl-4-morpholinothieno[3,2-*d*]pyrimidin-6-yl)methyl)piperazin-1-yl)-2-methylpropan-1-one (10**).** Compound **10** was prepared from intermediate **7** and *N*-Boc-aminoisobutyric acid by the procedure for compound **8** in 56% yield. ^1H NMR (400 MHz, DMSO) δ 9.18 (s, 2H), 8.12 (s, 3H), 7.09 (br s, 2H), 4.32 (br s, 2H), 4.03–3.91 (m, 4H), 3.90–3.53 (m, 4H), 2.93 (br m, 4H), 2.43 (s, 3H), 1.55 (s, 6H). MS: (ESI+) 512.1.

1-(4-((2-(2-Aminopyrimidin-5-yl)-7-methyl-4-morpholinothieno[3,2-*d*]pyrimidin-6-yl)methyl)piperazin-1-yl)-2-hydroxyethanone (11**).** Compound **11** was prepared from intermediate **7** and 2-hydroxyacetic acid by the procedure for compound **8** in 42% yield

but did not necessitate final Boc-deprotection prior to reverse phase HPLC purification. ^1H NMR (400 MHz, DMSO) δ 9.15 (s, 2H), 7.04 (s, 2H), 4.51 (t, $J = 5.5$ Hz, 1H), 4.07 (d, $J = 5.5$ Hz, 2H), 3.97–3.91 (m, 4H), 3.85 (s, 2H), 3.81–3.75 (m, 4H), 3.54–3.45 (m, 2H), 3.42–3.32 (m, 2H), 2.35 (s, 3H). MS: (ESI+) 485.3.

(5)-1-(4-((2-(2-Aminopyrimidin-5-yl)-7-methyl-4-morpholinothieno[3,2-*d*]pyrimidin-6-yl)methyl)piperazin-1-yl)-2-hydroxypropan-1-one (**2**). Compound **2** was prepared from intermediate **7** and L-lactic acid by the procedure for compound **11** in 87% yield. Chiral HPLC analysis for **2** was performed with a Chiral Technologies Chiralcel OJ-RH (4.6 mm \times 150 mm, 5 μm) column and found to be >99% enantiomerically pure (isocratic elution with 0.1% DEA in methanol (v/v), run time = 20 min, flow rate of 1.0 mL/min, detection = 270 nm, injection volume = 5 μL , $t_{\text{R}} = 5.8$ min, $t_{\text{R}} = 7.6$ min). ^1H NMR (400 MHz, DMSO-*d*₆) δ 1.18 (d, $J = 6.53$ Hz, 3H), 2.34 (s, 3H), 2.38–2.60 (br, 4H), 3.36–3.64 (br, 4H), 3.67–3.78 (m, 4H), 3.84 (s, 2H), 3.89–4.00 (m, 4H), 4.35–4.48 (m, 1H), 4.84 (d, $J = 6.98$ Hz, 1H), 7.05 (s, 2H), 9.15 (s, 2H). MS: (ESI+) 499.1.

(R)-1-(4-((2-(2-Aminopyrimidin-5-yl)-7-methyl-4-morpholinothieno[3,2-*d*]pyrimidin-6-yl)methyl)piperazin-1-yl)-2-hydroxypropan-1-one (**12**). Compound **12** was prepared from intermediate **7** and L-lactic acid by the procedure for compound **11** in 61% yield. ^1H NMR (400 MHz, DMSO) δ 9.15 (s, 2H), 7.02 (s, 2H), 4.81 (d, $J = 6.9$ Hz, 1H), 4.41 (dq, $J = 6.6$ Hz, 1H), 3.97–3.91 (m, 4H), 3.84 (s, 2H), 3.81–3.74 (m, 4H), 3.55–3.41 (br m, 4H), 2.55–2.41 (br m, 4H), 2.35 (s, 3H), 2.07 (s, 2H), 1.18 (d, $J = 6.5$ Hz, 3H). MS: (ESI+) 499.1.

1-(4-((2-(2-Aminopyrimidin-5-yl)-7-methyl-4-morpholinothieno[3,2-*d*]pyrimidin-6-yl)methyl)piperazin-1-yl)-2-hydroxy-2-methylpropan-1-one (**13**). Compound **13** was prepared from intermediate **7** and 2-hydroxy-2-methylpropanoic acid by the procedure for compound **11** in 54% yield. ^1H NMR (400 MHz, DMSO) δ 9.16 (s, 2H), 7.04 (s, 2H), 5.35 (s, 1H), 3.98–3.91 (m, 5H), 3.85–3.81 (m, 2H), 3.81–3.75 (m, 5H), 2.51–2.47 (m, 4H), 2.35 (s, 3H), 1.31 (s, 6H). MS: (ESI+) 513.3.

Characterization of Biochemical and Cellular Activity in Vitro. Enzymatic activity of the class I PI3K isoforms and human recombinant mTOR were measured using a fluorescence polarization assay as described previously.³¹ VPS34 and C2b were assayed using a scintillation proximity assay as described previously.¹⁶ DNA-PK was assayed using a capillary electrophoresis assay that monitors production of phosphorylated peptide as well as loss of unphosphorylated substrate. In a total volume of 5 μL , DNA-PK (2 units/ μL ; Promega) was incubated with 1.5 μM peptide substrate (5-FAM-AEPLSQEAFADLWKK-NH₂) in the presence of 10 mM Hepes (pH 7.2), 10 mM MgCl₂, 10 μM ATP, 10 $\mu\text{g}/\text{mL}$ calf thymus DNA, 0.015% (v/v) Brij-35, 1 mM dithiothreitol, and 2% dimethylsulfoxide.³⁶ After incubation for 60 min at 25 $^{\circ}\text{C}$ the reaction was terminated with a final concentration of 25 mM Hepes (pH 7.2), 0.0037% Brij-35, 37.5 mM EDTA. Dose–response curves were fit to an equation for tight-binding inhibition using the measured K_{m} for ATP for DNA-PK of 9.3 μM .

Kinase selectivity was measured using the SelectScreen service at Invitrogen (LifeTechnologies), profiling 145 or 240 kinases for % inhibition at 1 μM compound using the Z-lyte assay format or the Adapta assay format as specified by Lifetechnologies.

IC_{50} s were calculated from the fit of the dose–response curves to a four-parameter equation and were measured at the experimental K_{m} for ATP for the kinase of interest. Alternatively, apparent K_{S} were calculated by fitting the data to an equation for tight-binding inhibition as previously described.³¹

Antiproliferative cellular assays were conducted as described³¹ using PC3 and MCF7.1 human tumor cell lines provided by the ATCC or Genentech Research laboratories, respectively. MCF7.1 is an in vivo selected line developed at Genentech and originally derived from the parental human MCF7 breast cancer cell line (ATCC, Manassas, VA).

All IC_{50} or K_{iapp} values for both biochemical and cellular assays represent geometric means of multiple replicates or of duplicates. Biochemical assays typically showed <30% difference between duplicates or replicates and cellular assays were typically within 2-fold agreement between replicates.

In Vivo Xenograft Studies. Human prostate cancer PC3 cells obtained from the National Cancer Institute (Frederick, MD) were resuspended in Hank's Balanced Salt Solution and 3×10^6 cells implanted subcutaneously into the right hind flank of athymic nu/nu (nude) mice. Tumors were monitored until they reached a mean tumor volume of 150–200 mm^3 prior to the initiation of dosing. MCF7.1 cells resuspended in a 1:1 mixture of Hank's Buffered Salt Solution and Matrigel Basement Membrane Matrix (no. 356237, BD Biosciences; Santa Cruz, CA) were 5×10^6 subcutaneously implanted into the right hind flank of athymic nu/nu (nude) mice. Prior to cell inoculation, 17 β -estradiol (0.36 mg/pellet, 60-day release, no. SE-121) obtained from Innovative Research of America (Sarasota, FL) were implanted into the dorsal shoulder blade area of each nude mouse. After implantation of cells, tumors were monitored until they reached a mean tumor volume of 250–350 mm^3 prior to initiating dosing. Compound **2** was dissolved in 0.5% methylcellulose with 0.2% Tween-80 (MCT). Female nude (nu/nu) mice that were 6–8 weeks old and weighed 20–30 g were obtained from Charles River Laboratories (Hollister, CA). Tumor bearing mice were dosed daily for 14–21 days depending on the xenograft model with 100 μL of vehicle (MCT) or test agent orally.

Tumor volume was measured in two dimensions (length and width) using Ultra Cal-IV calipers (model 54–10–111; Fred V. Fowler Company; Newton, MA) and was analyzed using Excel version 11.2 (Microsoft Corporation; Redmond, WA). The tumor volume (mm^3) = (longer measurement \times shorter measurement²) \times 0.5. Animal body weights were measured using an Adventurer Pro AV812 scale (Ohaus Corporation; Pine Brook, NJ). Percent weight change = $[1 - (\text{new weight}/\text{initial weight})] \times 100$. Tumor sizes were recorded twice weekly over the course of the study (14–21 days). Mouse body weights were also recorded twice weekly, and the mice were observed daily. Mice with tumor volumes $\geq 2000 \text{ mm}^3$ or with losses in body weight $\geq 20\%$ from their initial body weight were promptly euthanized per IACUC guidelines. Mean tumor volume and SEM values ($n = 10$) were calculated using JMP statistical software, version 5.1.2 at end of treatment. % Tumor inhibition = $100(\text{mean volume of tumors in vehicle treated animals} - \text{mean volume of tumors in test article treated animals given the test article})/\text{mean volume of tumors in vehicle treated animals}$. Data were analyzed and *p*-values were determined using the Dunnett *t* test with JMP statistical software, version 5.1.2 (SAS Institute; Cary, NC).

Accession Codes

The coordinates and structure factors for compound **2** has been deposited (PDB code 3TL5).

AUTHOR INFORMATION

Corresponding Author

*Phone: 650-225-3171. Fax: 650-225-2061. E-mail: sutherland.dan@gene.com.

ACKNOWLEDGMENT

We thank Mengling Wong, Martin Struble, Yanzhou Liu, and Wen Chiu for compound purification and determination of purity by HPLC, mass spectroscopy, and ^1H NMR. We thank Krista K. Bowman, Alberto Estevez, Kyle Mortara, and Jiansheng Wu for technical assistance of protein expression and purification. We thank Emil Plise for plasma protein binding data. We are grateful to Michelle Nannini, Janeko Bower, and Alex Vanderbilt

for coordinating and dosing animals for the reported in vivo efficacy studies.

■ ABBREVIATIONS USED

AKT, protein kinase B; DCE, dichloroethane; DMF, dimethylformamide; DMSO, dimethylsulfoxide; EGFR, epidermal growth factor receptor 1; HATU, (2-(7-aza-1H-benzotriazole-1-yl)-1,1,3,3-tetramethyluronium hexafluorophosphate); HER2, epidermal growth factor receptor 2; PEG, polyethylene glycol; PI3K, phosphoinositide 3-kinase; PPB, plasma protein binding; PTEN, phosphatase and tensin homologue; mTOR, mammalian target of rapamycin; TFA, trifluoroacetic acid; THF, tetrahydrofuran

■ REFERENCES

- (1) Vivanco, L.; Sawyers, C. L. The phosphatidylinositol 3-kinase AKT pathway in human cancer. *Nature Rev. Cancer* **2002**, *2*, 489–501.
- (2) Cantley, L. C. The phosphoinositide 3-kinase pathway. *Science* **2002**, *296*, 1655–1657.
- (3) Vanhaesebroeck, B.; Guillermet-Guibert, J.; Graupera, M.; Bilanges, B. The emerging mechanisms of isoform-specific PI3K signaling. *Nature Rev. Mol. Cell Biol.* **2010**, *11*, 329–341.
- (4) Guertin, D. A.; Sabatini, D. M. Defining the role of mTOR in cancer. *Cancer Cell* **2007**, *12*, 9–22.
- (5) Laplante, M.; Sabatini, D. M. mTOR signaling at a glance. *J. Cell. Sci.* **2010**, *122*, 3589–3594.
- (6) Engelman, J. A. Targeting PI3K signaling in cancer: opportunities, challenges and limitations. *Nature Rev. Cancer* **2009**, *9*, 550–562.
- (7) Vilar, E.; Perez-Garcia, J.; Taberero, J. Pushing the Envelope in the mTOR Pathway: The Second Generation of Inhibitors. *Mol. Cancer Ther.* **2011**, *10*, 395–403.
- (8) Ihle, N. T.; Powis, G. Take your PIK: phosphatidylinositol 3-kinase inhibitors race through the clinic and toward cancer therapy. *Mol. Cancer Ther.* **2009**, *8*, 1–9.
- (9) Shayesteh, L.; Kuo, W. L.; Baldocchi, R.; Godfrey, T.; Collins, C.; Pinkel, D.; Powell, B.; Mills, G. B.; Gray, J. W. PIK3CA is implicated as an oncogene in ovarian cancer. *Nature Genet.* **1999**, *21*, 99–102.
- (10) Samuels, Y.; Wang, Z.; Bardelli, A.; Silliman, N.; Ptak, J.; Szabo, S.; Yan, H.; Gazdar, A.; Powell, S. M.; Riggins, G. J.; Willson, J. K.; Markowitz, S.; Kinzler, K. W.; Vogelstein, B.; Velculescu, V. E. High frequency of mutations of the PIK3CA gene in human cancers. *Science* **2004**, *30*, 554.
- (11) Parsons, D. W.; Wang, T. L.; Samuels, Y.; Bardelli, A.; Cummins, J. M.; DeLong, L.; Silliman, N.; Ptak, J.; Szabo, S.; Willson, J. K.; Markowitz, S.; Kinzler, K. W.; Vogelstein, B.; Lengauer, C.; Velculescu, V. E. Colorectal cancer: mutations in a signalling pathway. *Nature* **2005**, *436*, 792.
- (12) Karakas, B.; Bachman, K. E.; Park, B. H. Mutations of the PIK3CA oncogene in human cancers. *Br. J. Cancer* **2006**, *94*, 455–9.
- (13) Sulis, M. L.; Parsons, R. PTEN: from pathology to biology. *Trends Cell. Biol.* **2003**, *13*, 478–483.
- (14) Li, J.; Yen, C.; Liaw, D.; Podsypanina, K.; Bose, S.; Wang, S. I.; Puc, J.; Miliaresis, C.; Rodgers, L.; McCombie, R.; Bigner, S. H.; Giovanella, B. C.; Ittmann, M.; Tycko, B.; Hibshoosh, H.; Wigler, M. H.; Parsons, R. PTEN, a putative protein tyrosine phosphatase gene mutated in human brain, breast, and prostate cancer. *Science* **1997**, *275*, 1943–1947.
- (15) Berns, K.; Horlings, H. M.; Hennessy, B. T.; Madiredjo, M.; Hijmans, E. M.; Beelen, K.; Linn, S. C.; Gonzalez-Angulo, A. M.; Stemke-Hale, K.; Hauptmann, M.; Beijersbergen, R. L.; Mills, G. B.; van de Vijver, M. J.; Bernards, R. A functional genetic approach identifies the PI3K pathway as a Major Determinant of Trastuzumab resistance in breast cancer. *Cancer Cell* **2007**, *12*, 395–402.
- (16) Folkes, A. J.; Ahmadi, K.; Alderton, W. K.; Alix, S.; Baker, S. J.; Box, G.; Chuckowree, I. S.; Clarke, P. A.; Depledge, P.; Eccles, S. A.; Friedman, L. S.; Hayes, A.; Hancox, T. C.; Kugendradas, A.; Lensun, L.; Moore, P.; Olivero, A. G.; Pang, J.; Patel, S.; Pergl-Wilson, G. H.; Raynaud, F. I.; Robson, A.; Saghir, N.; Salphati, L.; Sohail, S.; Ultsch, M. H.; Valenti, M.; Wallweber, H. J. A.; Wan, N. C.; Wiesmann, C.; Workman, P.; Zhyvoloup, P.; Zvelebil, M. J.; Shuttleworth, S. J. The Identification of 2-(1H-Indazol-4-yl)-6-(4-methanesulfonyl-piperazin-1-ylmethyl)-4-morpholin-4-yl-thieno[3,2-d]pyrimidine (GDC-0941) as a Potent, Selective, Orally Bioavailable Inhibitor of Class I PI3 Kinase for the Treatment of Cancer. *J. Med. Chem.* **2008**, *51*, 5522–5532.
- (17) Salphati, L.; Wong, H.; Belvin, M.; Bradford, D.; Edgar, K. A.; Prior, W. W.; Sampath, D.; Wallin, J. J. Pharmacokinetic–pharmacodynamic modeling of tumor growth inhibition and biomarker modulation by the novel phosphatidylinositol 3-kinase inhibitor GDC-0941. *Drug. Metab. Dispos.* **2010**, *38*, 1436–1442.
- (18) Lannutti, B. J.; Meadows, S. A.; Herman, S. E. M.; Kashishian, A.; Steiner, B.; Johnson, A. J.; Byrd, J. C.; Tyner, J. W.; Loriaux, M. M.; Deininger, M.; Druker, B. J.; Puri, K. J.; Ulrich, R. G.; Giese, N. A. CAL-101, a p110delta selective phosphatidylinositol-3-kinase inhibitor for the treatment of B-cell malignancies, inhibits PI3K signaling and cellular viability. *Blood* **2011**, *117*, 591–594.
- (19) Rini, B. I. Temsirolimus, an Inhibitor of Mammalian Target of Rapamycin. *Clin. Cancer Res.* **2008**, *14*, 1286–1290.
- (20) Sarbassov, D. D.; Guertin, D. A.; Ali, S. M.; Sabatini, D. M. Phosphorylation on regulation of AKT/PKB by the Rictor-mTOR complex. *Science* **2005**, *307*, 1098–1101.
- (21) O'Reilly, K. E.; Rojo, F.; She, Q.-B.; Solit, D.; Mills, G. B.; Smith, D.; Lane, H.; Hofmann, F.; Hicklin, D. J.; Ludwig, D. L.; Baselga, J.; Rosen, N. mTOR inhibition induces upstream receptor tyrosine kinase signaling and activates Akt. *Cancer Res.* **2006**, *66*, 1500–1508.
- (22) Taberero, J.; Rojo, F.; Calvo, E.; Burris, H.; Judson, I.; Hazell, K.; Martinelli, E.; Ramon y Cajal, S.; Jones, S.; Vidal, L.; Shand, N.; Macarulla, T.; Ramos, F. R.; Dimirijevic, S.; Zoellner, U.; Tang, P.; Stumm, M.; Lane, H. A.; Leubwohl, D.; Baselga, J. Dose- and Schedule-Dependent Inhibition of the Mammalian Target of Rapamycin Pathway With Everolimus: A Phase I Tumor Pharmacodynamic Study in Patients With Advanced Solid Tumors. *J. Clin. Oncol.* **2008**, *26*, 1603–1610.
- (23) Tamburini, J.; Chapuis, N.; Bardet, V.; Park, S.; Sujobert, P.; Willems, L.; Ifrah, N.; Dreyfus, F.; Mayeux, P.; Lacombe, C.; Bouscary, D. Mammalian target of rapamycin (mTOR) inhibition activates phosphatidylinositol 3-kinase/Akt by up-regulating insulin-like growth factor-1 receptor signaling in acute myeloid leukemia: rationale for therapeutic inhibition of both pathways. *Blood* **2008**, *111*, 379–382.
- (24) Guertin, D. A.; Sabatini, D. M. The pharmacology of mTOR inhibition. *Sci. Signaling* **2009**, *2*, pe24 1–6.
- (25) Fasolo, A.; Sessa, C. mTOR inhibitors in the treatment of cancer. *Expert Opin. Invest. Drugs* **2008**, *17*, 1717–1734.
- (26) Maira, S.-M.; Stauffer, F.; Brueggem, J.; Furet, P.; Schnell, C.; Fritsch, C.; Brachmann, S.; Chene, P.; De Pover, A.; Schoemaker, K.; Fabbro, D.; Gabriel, D.; Simonen, M.; Murphy, L.; Finan, P.; Sellers, W.; Garcia-Echeverria, G. Identification and characterization of NVP-BEZ235, a new orally available dual phosphatidylinositol 3-kinase/mammalian target of rapamycin inhibitor with potent in vivo antitumor activity. *Mol. Cancer Ther.* **2008**, *7*, 1851–1863.
- (27) Knight, S. D.; Adams, N. D.; Burgess, J. L.; Chaudhari, A. M.; Darcy, M. G.; Donatelli, C. A.; Luengo, J. I.; Newlander, K. A.; Parish, C. A.; Ridgers, L. H.; Sarpong, M. A.; Schmidt, S. J.; Van Aller, G. S.; Carlson, J. D.; Diamond, M. A.; Elkins, P. A.; Gardiner, C. M.; Garver, E.; Gilbert, S. A.; Gontarek, R. R.; Jackson, J. R.; Kershner, K. L.; Luo, L.; Raha, K.; Sherk, C. S.; Sung, C.-M.; Sutton, D.; Tummino, P. J.; Wegrzyn, R. J.; Auger, K. R.; Dhanak, D. Discovery of GSK2126458, a Highly Potent Inhibitor of PI3K and the Mammalian Target of Rapamycin. *ACS Med. Chem. Lett.* **2010**, *1*, 39–43.
- (28) Dehnhardt, C. M.; Venkatesan, A. M.; Santos, E. D.; Chen, Z.; Santos, O.; Ayril-Kaloustain, S.; Brooijmans, N.; Mallon, R.; Hollander, I.; Feldberg, L.; Lucas, J.; Chaudhary, I.; Yu, K.; Gibbons, J.; Abraham, R.; Mansour, T. S. Lead Optimization of N-3-Substituted 7-Morpholino-triazolopyrimidines as Dual Phosphoinositide 3-Kinase/Mammalian Target of Rapamycin Inhibitors: Discovery of PKI-402. *J. Med. Chem.* **2010**, *53*, 798–810.

(29) Venkatesan, A. M.; Dehnhardt, C. M.; Santos, E. D.; Chen, Z.; Santos, O.; Ayrál-Kaloustain, Khafizova, G.; Brooijmans, N.; Mallon, R.; Hollander, I.; Feldberg, L.; Lucas, J.; Yu, K.; Gibbons, J.; Abraham, R.; Chaudhary, I.; Mansour, T. S. Bis(morpholino-1,3,5-triazine) Derivatives: Potent Adenosine 50-Triphosphate Competitive Phosphatidylinositol-3-kinase/Mammalian Target of Rapamycin Inhibitors: Discovery of Compound 26 (PKI-587), a Highly Efficacious Dual Inhibitor. *J. Med. Chem.* **2010**, *53*, 2636–2645.

(30) Fan, Q.-W.; Knight, Z. A.; Goldenberg, D. D.; Yu, W.; Mostov, K. E.; Stokoe, D.; Shokat, K. M.; Weiss, W. A. A dual PI3 kinase/mTOR inhibitor reveals emergent efficacy in glioma. *Cancer Cell* **2006**, *9*, 341–349.

(31) Sutherlin, D. P.; Sampath, D.; Berry, M.; Castanedo, G.; Chang, Z.; Chuckowree, I.; Dotson, J.; Folkes, A.; Friedman, L.; Goldsmith, R.; Heffron, T.; Lee, L.; Lesnick, J.; Lewis, C.; Mathieu, S.; Nonomiya, J.; Olivero, A.; Pang, J.; Prior, W. W.; Salphati, L.; Sideris, S.; Tian, Q.; Tsui, V.; Wan, N. C.; Wang, S.; Wiesmann, C.; Wong, S.; Zhu, B.-Y. Discovery of (Thienopyrimidin-2-yl)aminopyrimidines as Potent, Selective, and Orally Available Pan-PI3-Kinase and Dual Pan-PI3-Kinase/mTOR Inhibitors for the Treatment of Cancer. *J. Med. Chem.* **2010**, *53*, 1086–1097.

(32) Heffron, T. P.; Berry, M.; Castanedo, G.; Chang, C.; Chuckowree, I.; Dotson, J.; Folkes, A.; Gunzner, J.; Lesnick, J. D.; Lewis, C.; Mathieu, S.; Nonomiya, J.; Olivero, A.; Pang, J.; Peterson, D.; Salphati, L.; Sampath, D.; Sideris, S.; Sutherlin, D. P.; Tsui, V.; Wan, N. C.; Wang, S.; Wong, S.; Zhu, B. Y. Identification of GNE-477, a Potent and Efficacious Dual PI3K/mTOR Inhibitor. *Bioorg. Med. Chem. Lett.* **2010**, *20*, 2408–2411.

(33) Castanedo, G.; Dotson, J.; Goldsmith, R.; Gunzner, J.; Heffron, T.; Mathieu, S.; Olivero, A.; Staben, S.; Sutherlin, D. P.; Tsui, V.; Wang, S.; Zhu, B.-Y.; Bayliss, T.; Chuckowree, I.; Folkes, A.; Wan, N. C. Patent WO2008/073785 A2. 2008.

(34) Gleeson, M. P. Generation of a Set of Simple, Interpretable ADMET Rules of Thumb. *J. Med. Chem.* **2008**, *51*, 817–834.

(35) Obach, R. S.; Baxter, J. G.; Liston, T. E.; Silber, B. M.; Jones, B. C.; MacIntyre, F.; Rance, D. J.; Wastall, P. The prediction of human pharmacokinetic parameters from preclinical and in vitro metabolism data. *J. Pharmacol. Exp. Ther.* **1997**, *283*, 46–58.

(36) PK/PD studies were performed in tumor bearing animals at doses similar to those used in the PC3 xenograft efficacy study and showed evidence of pharmacologic inhibition of the pathway. At a 5 and 10 mg/kg doses, pAKT was reduced to 385% of vehicle control at all time points up to 8 h and 63% and 78% of vehicle control at 24 h with unbound plasma concentrations of 0.05 mM and 0.45 mM, respectively. A more detailed account of PK/PD and efficacy of this molecule is forthcoming.